



## Letter

## Effect of air contamination on ball milling and cold rolling of magnesium hydride

S.D. Vincent, J. Huot\*

*Institut de Recherche sur l'Hydrogène, Université du Québec à Trois-Rivières, 3351 Boul. des Forges, Trois-Rivières, Québec, Canada G9A 5H7*

## ARTICLE INFO

## Article history:

Received 17 February 2011

Accepted 24 February 2011

Available online 3 March 2011

## Keywords:

Hydrogen storage materials

Magnesium

Ball milling

Air contamination

Cold rolling

## ABSTRACT

In this letter we address the problem of air contamination in high energy milling and cold rolling of magnesium hydride. We found that for short milling time (30 min) milling under argon or air leads to the same crystal structure and same hydrogen sorption behaviour. In the case of the cold rolled sample, the hydrogen sorption behaviour is similar but the crystal structure shows some differences with ball milled samples. As expected, prolonged milling time in air leads to formation of magnesium oxide and degradation of hydrogen sorption capacities. However, kinetics do not seem to show degradation. This investigation shows that, for short milling time, air contamination is not as detrimental as was expected.

© 2011 Elsevier B.V. All rights reserved.

## 1. Introduction

Despite its high temperature of operation and slow hydrogen sorption kinetics, magnesium is still considered as a candidate for some hydrogen storage applications. In the search of magnesium and magnesium-based compounds with enhanced hydrogen storage properties, ball milling has been extensively used [1–8]. Usually, ball-milling is performed in argon or hydrogen atmosphere at different pressures. In either case, care is always made to ensure that the milling atmosphere is not contaminated with air. However, in the perspective of large scale utilization of this technique by the industry, the requirement of having a laboratory-grade atmosphere of argon or hydrogen may greatly add to the construction and operation costs.

Recently we have shown that cold rolling is effective in obtaining nanocrystallinity and enhancement of hydrogen sorption kinetics of magnesium hydride [9]. A potential advantage of this technique is that all operations (handling, rolling and storage) were made in air. For a small number of rolls, in that case five, the hydrogen capacity loss was found to be minimal and the hydrogen sorption kinetics almost as fast as for the same hydride milled 1 h. As cold rolling is extensively applied in the industry, it may be a good candidate for synthesis and preparation of metal hydrides. However, more practical knowledge of the effect of cold rolling on metal hydrides has to be investigated.

In this letter we present an investigation on the effect of air on the hydrogen storage behaviour of material processed by cold rolling and ball milling. In our first study cold rolling was carried out in air while ball milling was performed in argon [9]. In order to truly compare these two methods the processing has to be under the same atmosphere. As air contamination is always a concern when ball milling is done in protective atmosphere such as argon, we decided to elucidate this problem by performing all handling and processing in air. As this is the most drastic conditions that could be encountered, this type of study will establish a 'worst case scenario' for both methods.

We present here the crystal structure and hydrogen storage performances of magnesium hydride that has been cold rolled or ball milled in air. They are compared with magnesium hydride ball milled under standard conditions in argon.

## 2. Experimental method

The cold-rolling apparatus used in this study was a Durston DRM 130 modified in such a way that vertical milling is possible. This configuration enables the processing of powder samples. As starting material we used 300 mesh  $\text{MgH}_2$  powder (98% purity) from Alfa Aesar. Cold rolling was performed by inserting the powder mixtures between two 316 stainless steel plates to prevent contamination from the rolls. All rollings were performed in air. After each rolling pass, the powder was collected and rolled again to the final numbers of rolls. Milling was carried out on a Spex 8000 high energy mill in a hardened steel crucible with a powder to ball ratio of 1/10. For millings performed in air the crucible was loaded with powders and closed in ambient air. After each milling time the crucible was open in air, a small sample collected and the crucible was closed in air before resuming milling. As a comparison, milling under argon was carried out. In that case all handlings, loading and closing of crucible were made in an argon atmosphere glove box.

The hydrogen sorption properties were measured with a Sieverts-type apparatus. All measurements were performed at 623 K with a hydrogen pressure of

\* Corresponding author. Tel.: +1 819 376 5011; fax: +1 819 376 5164.

E-mail address: [jacques.huot@uqtr.ca](mailto:jacques.huot@uqtr.ca) (J. Huot).

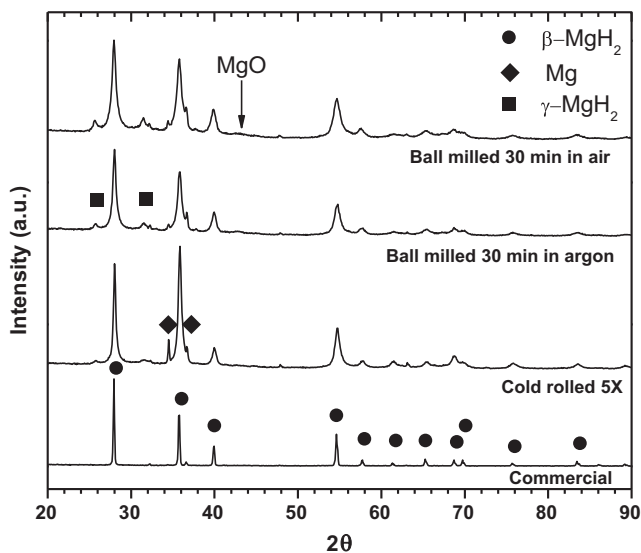


**Fig. 1.** X-ray powder diffraction of  $\text{MgH}_2$  in its as-received state, after 5 cold rolled, after 30 min of ball milling in argon and after 30 min of ball milling in air. Arrow indicates the position of the most intense Bragg peak of  $\text{MgO}$ .

2000 kPa for absorption and 35 kPa for desorption. Crystal structure was analyzed from X-ray powder diffraction patterns registered on a Bruker D8 Focus apparatus with  $\text{CuK}\alpha$  radiation. Phases abundances as well as crystallite size and microstrain were evaluated from Rietveld method using Topas software [10] via the fundamental parameters approach [11].

### 3. Results

#### 3.1. Crystal structure

Fig. 1 shows the X-ray powder diffraction patterns of commercial  $\text{MgH}_2$  in its as-received form as well as after five cold rollings in air, ball milled for 30 min in air and ball milled for 30 min in argon. As shown in our previous study, cold rolling five times is almost as effective as ball milling 30 min to obtain a nanocrystalline structure. The striking result here is that the powder diffraction pattern of the sample ball milled in air is practically identical to the sample ball milled in argon. As an indication, the most intense Bragg peak of  $\text{MgO}$  (periclase) is marked on the figure. There is no visual indication for the formation of oxide in any patterns. To get a quantitative interpretation, we performed Rietveld refinement on these patterns. In Table 1 we present the phase abundance as evaluated from Rietveld refinement. It should be pointed out that in order to get a better fit, in the refinements of cold rolled and ball milled samples a broad single peak centered around  $32^\circ$  was included. As we used some grease to stick the powder to the sample holder for X-ray diffraction measurement, this is probably the origin of this amorphous structure. In computation of relative abundance, only crystalline phases were taken into account.

In the case of commercial  $\text{MgH}_2$  the 3 wt.% of magnesium agrees well with the manufacturer claim of 98% pure  $\text{MgH}_2$ . Within experimental uncertainties this value is the same for all samples. Table 1 also shows that the metastable phase  $\gamma\text{-MgH}_2$  is formed by cold

**Table 1**  
Phases abundances in wt.% as evaluated from Rietveld refinement. Error on all values is  $\pm 1$ . For some samples total do not add to 100 because of round-off.

	Commercial	CR5X	BM 30 min air	BM 30 min argon
Mg	3	3	3	3
$\beta\text{-MgH}_2$	97	83	81	81
$\gamma\text{-MgH}_2$	–	5	8	9
$\text{MgO}$	–	9	7	7

rolling and ball milling. It is already well known that  $\gamma\text{-MgH}_2$  could be synthesized by ball milling [1,12]. The interesting fact here is that atmosphere of milling is not important (at least for short milling duration) as the amount of  $\gamma\text{-MgH}_2$  phase is similar for samples milled in air and argon. Another interesting fact is that with only 5 cold-rollings the  $\gamma\text{-MgH}_2$  phase is already synthesized. As already mentioned in Ref. [9], it takes only 10 s to perform 5 cold roll. Therefore, cold rolling is a very efficient way to synthesize  $\gamma\text{-MgH}_2$  phase.

Rietveld refinement shows that magnesium oxide is present in all ball-milled and cold rolled samples in the same quantity. First, it should be pointed out that the oxide phase is hard to see on the diffraction pattern because the peaks are very broad due to the very small crystallite size as determined from Rietveld refinement (about 4 nm for all samples). Such a small crystallite size for magnesium oxide is expected as shown by Fournier et al. who found that the thickness of the oxides formed during oxidation between room temperature and 673 K varies from 1.5 to 4.3 nm [13]. Therefore, the crystallite size found from our Rietveld refinement could be considered as reasonable. Secondly, the surprising fact is that the oxide abundance is the same even for the sample that was processed in argon. Obviously, the reason could not be contamination of argon atmosphere because in this case the oxide content would be much higher for the sample processed in air. One may argue that because of the very broad peak the oxide phase is actually just fitting some background and the identification of periclase is an artefact. This is probably not the case because, as will be shown later, the oxide abundance clearly increases with ball milling time. However, the fact that oxide is also present in the sample ball milled in argon has to be explained. For this, the amount of air exposure of each sample has to be clearly stated. In the case of cold rolled sample, it was always kept and process in air. Therefore, for this sample the amount of oxygen available for oxidation is effectively infinite. From the crucible volume, we estimated that during milling a maximum of 2.6 wt.% of magnesium will be oxidized. This is a factor 3 lower than what we measured from Rietveld analysis. Finally, the sample milled in argon is always handled in the glove box therefore the air exposure of this sample should be minimal (a few ppm). As mentioned above, magnesium oxide forms surface layers from 1 to 4 nm. Such small crystallite size produce very broad peaks that, combined with a small intensity due to the low oxide content, may be very difficult to detect in the as-received powder. To test this hypothesis we ball milled  $\text{MgH}_2$  for 10 h in argon atmosphere with all handling in an argon glove box. The X-ray powder diffraction was taken with a sealed sample holder in order to never expose the sample to air. After completion of the diffraction pattern, the protecting dome of the sample holder was taken out in order to expose the powder to the air without changing anything else. After a few hours of air exposure another diffraction pattern was registered. Fig. 2 shows the two diffraction patterns. The diffraction pattern before exposition to the air (with dome) presents a high background at low angles. This is due to the presence of the protective dome. After removal of the dome for air exposure this background totally disappears. It is clear that air exposure lead to formation of  $\text{MgO}$ . Quantitative evaluation of phases abundances was made by performing Rietveld refinement on both patterns. Before air exposure (pattern with dome) the respective abundance (in wt.%) of  $\beta\text{-MgH}_2$ ,  $\gamma\text{-MgH}_2$ , and  $\text{MgO}$  was 70%, 25%, and 5%. As the  $\text{MgO}$  abundance agrees with the value determined for the ball milled and cold rolled samples, we could conclude that about 5 wt.% of  $\text{MgO}$  is originally present in  $\text{MgH}_2$  commercial powder. After air exposure (pattern without dome) the respective abundances of  $\beta\text{-MgH}_2$ ,  $\gamma\text{-MgH}_2$ , and  $\text{MgO}$  were 56%, 23%, and 22%. As expected the  $\text{MgO}$  content drastically increased but the interesting observation is that the abundance of the metastable phase  $\gamma\text{-MgH}_2$  is essentially constant. This is a perplexing result because one would expect that

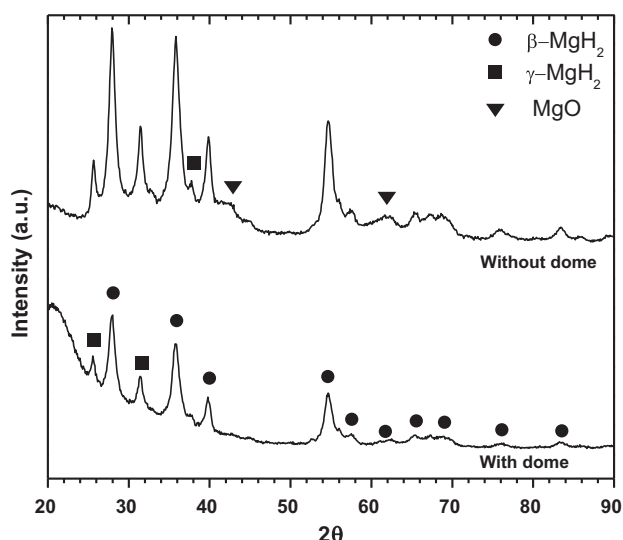


**Fig. 2.** X-ray powder diffraction of  $\text{MgH}_2$  ball milled 10 h in argon atmosphere. With dome = before air exposure, without dome = after air exposure.

the first phase to react with oxygen to form an oxide would be the metastable phase  $\gamma\text{-MgH}_2$  while in fact this phase is stable and it is the  $\beta\text{-MgH}_2$  abundance which decreases proportionally to the increase of MgO. One tentative explanation may be that, as the  $\gamma\text{-MgH}_2$  phase is due to micro-stress relaxation [14] it is probably located not on the surface of particles but deep in its interior. Thus, as oxidation takes place on the surface it will be preferentially the  $\beta\text{-MgH}_2$  phase that will decompose, leaving the  $\gamma\text{-MgH}_2$  phase intact in the interior.

Going back to Fig. 1 and Table 1 we could have now a better interpretation of these results. Taking the amount of oxide in the raw powders as 5 wt.% and adding the amount of air in the crucible (about 2.6 wt.%) one get a value of 7.6 wt.% which is very close to the value recorded for the 30 min ball milled in air of Table 1. In the case of the sample milled 30 min in argon, the oxide abundance of 7 wt.% may be explained by the fact that this pattern was registered using a sample holder open to the air. We thus think that the powder reacted in situ with air in a similar way as for the 10 h ball milled in argon presented in Fig. 2. The higher oxide abundance of the cold rolled sample could be explained by the fact that this powder is more reactive than the corresponding 30 min milled sample and thus could oxidized to a higher degree. The essential fact to point out here is that oxidation do not seems to depend so much on the time of air exposure but more on the reactivity of the powder. If a highly reactive powder such as nanocrystalline powder produce by cold rolling or milling, is exposed to the air even for a short period of time then oxidation will occur. Once the surface of the grain is covered by oxide the oxidation will stop and oxide content will stay constant.

Beside oxide abundance, other features are interesting to consider. From Rietveld refinement crystallite size and microstrain could be evaluated. As the abundances of magnesium and  $\gamma\text{-MgH}_2$  phases are relatively low, accurate measurement of crystallite size and microstrain is difficult for them. Therefore, crystallite size and microstrain of only  $\beta\text{-MgH}_2$  phase are reported in Table 2. As expected, commercial  $\text{MgH}_2$  has a large crystallite size and relatively small microstrain. Upon ball milling, crystallite size is reduced and microstrain increases. It is interesting to note that crystallite size is smaller and microstrain bigger when milling is done in air than when it is in argon. Moreover, the sample that was cold rolled also shows an important reduction of crystallite size and a high value of microstrain.

**Table 2**

Crystallite size and microstrain of the  $\beta\text{-MgH}_2$  phase. Values in parenthesis are uncertainties on the last significant digit.

	Commercial	CR5X	BM 30 min Air	BM 30 min Argon
Crystallite size (nm)	184(3)	25.4(7)	16.7(4)	18.5(4)
Microstrain (%)	0.190(4)	0.71(3)	0.95(4)	0.75(4)

From Table 2 we see that cold rolling is almost as effective in reduction of crystallite size as ball milling. Despite the fact that crystallite size and microstrain are similar for cold rolled and ball milled samples, some important discrepancies are seen. Close inspection of Fig. 1 shows that, for the cold rolled sample the  $\beta\text{-MgH}_2$  phase shows a texture along (0 1 1). Moreover, the magnesium phase is also textured along (0 0 2), the *c* axis of the hexagonal lattice. Ball milled samples did not show any texture. Thus, despite the fact that cold rolling is as efficient as ball milling in obtaining a nanocrystalline structure, there is fundamental discrepancies between these two methods.

### 3.2. Hydrogen sorption properties

The hydrogen absorption kinetics at 623 K and under hydrogen pressure of 2000 kPa for commercial, cold rolled and ball-milled samples are shown in Fig. 3. In the case of commercial  $\text{MgH}_2$  without any treatment the kinetic is slow, reaching only 50% of maximum capacity after 250 s. The main fact is that the three other samples have very similar kinetics. This likeness in hydrogen absorption agrees with the similar crystal structures measured from X-ray powder diffraction.

Desorption kinetics are shown in Fig. 4. As for absorption, we see that the commercial alloy has slow kinetics while the three processed samples have similar kinetics and hydrogen capacities. A closer inspection shows that actually the main difference between the commercial and processed samples is the incubation time before desorption really starts. At mid-reaction (around 0.4 and 0.5 of reacted fraction) the slope is almost the same for all samples. This means that for desorption the main difference is that the processed magnesium hydrides have more nucleation points than the as-received  $\text{MgH}_2$ . These nucleation points are coming from

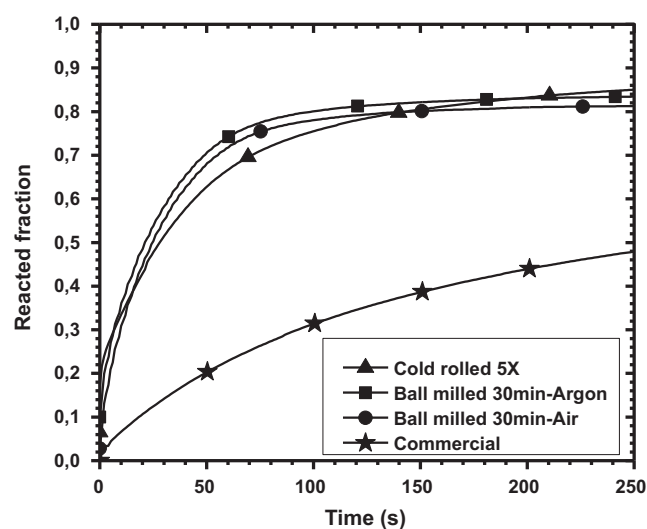


**Fig. 3.** Hydrogen absorption kinetics at 623 K under 2000 kPa of hydrogen. Capacities are expressed as fraction of theoretical maximum capacity (7.6 wt.%). Data points were taken at every second. Symbols are shown only for curves identification.

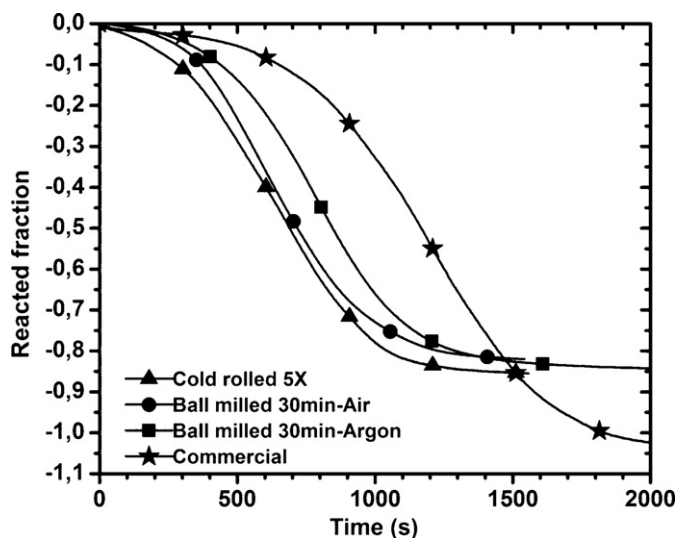


**Fig. 4.** Hydrogen desorption kinetics at 623 K under 35 kPa of hydrogen. Capacities are expressed as fraction of theoretical maximum capacity (7.6 wt.%). Data points were taken at every second. Symbols are shown only for curves identification.

the nanocrystalline structure and the number of defects introduced during milling or cold rolling.

For practical applications, desorption pressure should be of the order of 1 bar instead of vacuum [15]. Thus, we also measured the desorption kinetics at 350 °C under 1 bar of hydrogen. Results presented in Fig. 5 show that, as expected, the desorption kinetics are much slower for all samples. The interesting result is that even if the cold rolled sample has slower kinetic than the ball milled ones, the desorption is more complete.

In any case, the important point here is the comparison between the different processes and it is clear that ball milling in air does not significantly change the kinetics or the hydrogen capacity. On the other hand, this is only for a relatively short milling time. In order to have a better understanding on the effect of milling in air, much longer milling time should be investigated.

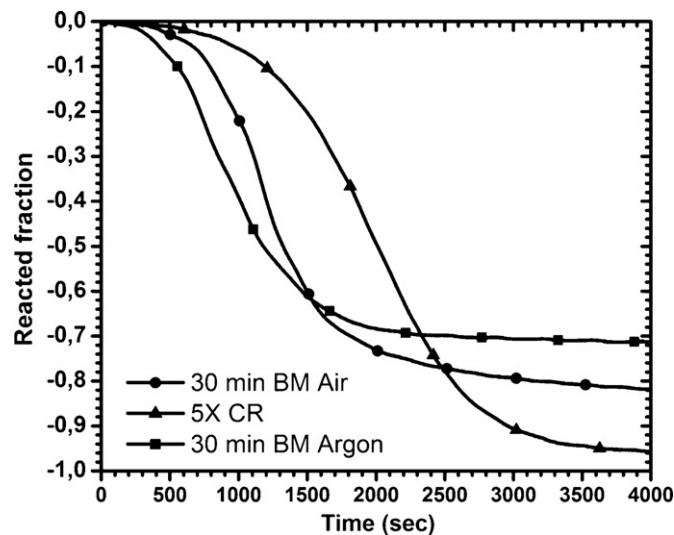


**Fig. 5.** Hydrogen desorption kinetics at 623 K under 100 kPa of hydrogen. Capacities are expressed as fraction of theoretical maximum capacity (7.6 wt.%). Data points were taken at every second. Symbols are shown only for curves identification.

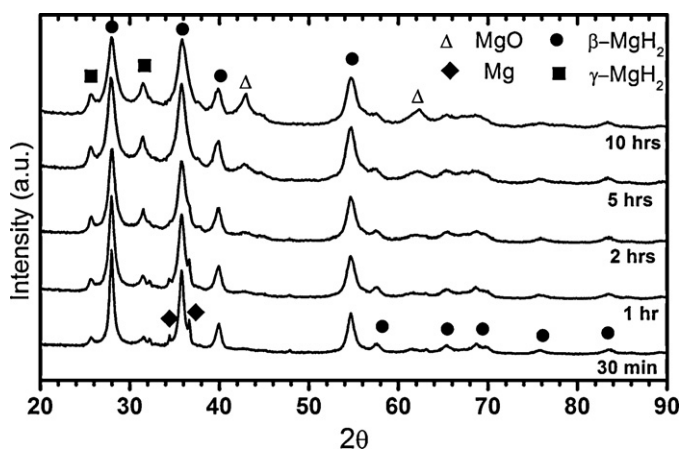


**Fig. 6.** X-ray powder diffraction of MgH<sub>2</sub> after 30 min, 1 h, 2 h, 5 h, and 10 h of ball milling in air.

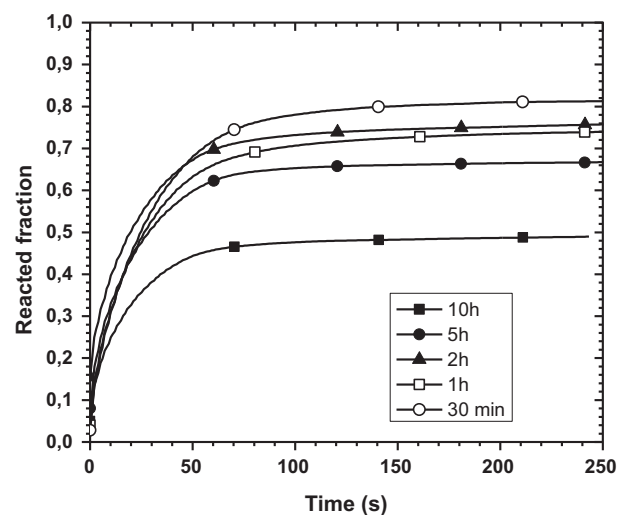


**Fig. 7.** Hydrogen absorption kinetics at 623 K under 2000 kPa of hydrogen. Capacities are expressed as fraction of theoretical maximum capacity (7.6 wt.%). Data points were taken at every second. Symbols are shown only for curves identification.

### 3.3. Effect of milling time on crystal structure

The effect of milling time was investigated with samples milled for 30 min, 1, 2, 5 and 10 h. As samples were taken at each milling time, it means that for the sample milled 10 h the crucible was open 4 times (after 30 min, 1, 2, and 5 h). In this way, air was reintroduced at certain times during the process and that if oxidation takes place there will be enough 'fresh' air to oxidize the material. The X-ray powder diffractions of these samples are presented in Fig. 6 and their phases abundances are shown in Table 3. As expected the abundance of magnesium oxide goes up with milling time while the one for magnesium goes down. However, as calculated in Section 3.1, each filling of air should bring about 2.6 wt.% of increase in magnesium oxide. Thus, for the 10 h ball milled the total amount of

**Table 3**

Phases abundances in wt.% as evaluated from Rietveld refinement. Error on all values is  $\pm 1$ . For some samples total do not add to 100 because of round-off.

	30 min	1 h	2 h	5 h	10 h
Mg	3	3	2	0	1
$\beta$ -MgH <sub>2</sub>	81	79	74	70	64
$\gamma$ -MgH <sub>2</sub>	8	10	12	12	11
MgO	7	9	12	17	24



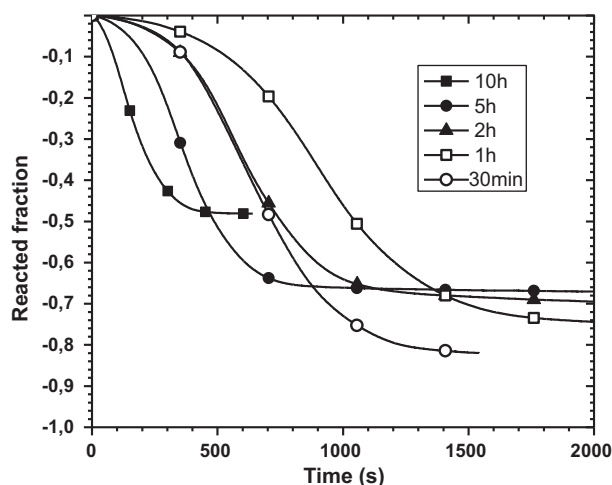


**Fig. 8.** Hydrogen desorption kinetics at 623 K under 35 kPa of hydrogen. Capacities are expressed as fraction of theoretical maximum capacity (7.6 wt.%). Data points were taken at every second. Symbols are shown only for curves identification.

oxide should be the oxide in the original powder (5 wt.%) plus the one due to filling of air  $5 \times 2.6$  wt.% for a total of about 18 wt.%. The amount found from Rietveld refinement is higher at 24 wt.%. However, the amount of oxide of the powder ball milled in argon and exposed to the air was found to be 22 wt.% (see Section 3.1). Therefore, it seems that it is the exposure to the air itself and not the fact of milling that is important. A powder milled in argon and exposed to the air seems to have the same characteristic as a powder milled in air.

### 3.4. Effect of milling time on hydrogen sorption properties

Fig. 7 shows the absorption kinetics of air-milled  $\text{MgH}_2$  for different milling times. As expected, the capacity decreases with milling time with the exception of a small reversal for the 1 and 2 h milling time but this is within experimental error. On the other hand, despite reduction of total capacity, the hydrogenation kinetic do not seems to vary with milling time. Therefore, it seems that the presence of magnesium oxide do not have any impact on the intrinsic kinetic of the remaining  $\text{MgH}_2$  phase.

Desorption kinetics are presented on Fig. 8. The loss of capacity seen on absorption (Fig. 7) is confirmed. However, we see that, except for the 1 h milled, there is a general trend of faster kinetics with milling time. This kinetic improvement is due to two factors: (1) a slight increases of intrinsic kinetic (steeper slope at mid dehydrogenation) and (2) a reduction of incubation time with milling time. Reduction of incubation time could be attributed to

the increasing number of defects with increasing milling time. In the present case, formation of oxide during milling do not seems to have a detrimental effect on sorption kinetics except reduction of total capacity.

## 4. Conclusion

This investigation of the effects of air exposure and milling in air showed that the main consequence is reduction of hydrogen capacity due to formation of oxide. A nanocrystalline structure is as easily obtained by milling in air as by milling in argon. Moreover, synthesis of the metastable  $\gamma\text{-MgH}_2$  phase is also possible by milling in air. Formation of  $\text{MgO}$  preferentially from  $\beta\text{-MgH}_2$  seems to indicate that  $\gamma\text{-MgH}_2$  phase is not on the surface of particles. Despite a diminution of total hydrogen capacity the air-milled samples showed an improvement of hydrogen sorption kinetics with milling time. In fact, for short milling time the kinetic of air-milled and argon milled  $\text{MgH}_2$  are similar. This investigation shows that, for short milling time, air contamination is not very detrimental in term of hydrogen capacity and kinetics. Long milling time in air will reduce capacities but do not have an important impact on the kinetics.

## Acknowledgements

This work was funded by the Natural Sciences and Engineering Research Council of Canada (NSERC). S.D. Vincent would like to thanks Hydro-Québec for a summer fellowship.

## References

- [1] J. Huot, et al., *Journal of Alloys and Compounds* 293–295 (1999) 495–500.
- [2] G. Liang, et al., *Journal of Alloys and Compounds* 292 (1999) 247–252.
- [3] M. Dornheim, et al., *Scripta Materialia* 56 (2007) 841–846.
- [4] A. Vaichere, et al., *Materials Science Forum* 570 (2008) 39–44.
- [5] W. Oelerich, T. Klassen, R. Bormann, *Journal of Alloys and Compounds* 315 (2001) 237–242.
- [6] J.F.R.d. Castro, et al., *Journal of Alloys and Compounds* 389 (2005) 270–274.
- [7] N. Hanada, T. Ichikawa, H. Fujii, *Journal of Alloys and Compounds* 446–447 (2007) 67–71.
- [8] I. Zavalii, R. Denys, V. Berezovets, *Materials Science* 45 (2) (2009) 248–257.
- [9] J. Lang, J. Huot, *Journal of Alloys and Compounds* 509 (3) (2011) L18–L22.
- [10] AXS, B., TOPAS V4: General profile and structure analysis software for powder diffraction data, 2008: Karlsruhe, Germany.
- [11] R.W. Cheary, A.A. Coelho, J.P. Cline, *Journal of Research of the National Institute of Standard and Technology* 109 (1) (2004) 1–25.
- [12] P. Wang, et al., *Journal of Alloys and Compounds* 313 (2000) 209–213.
- [13] V. Fournier, P. Marcus, I. Olefjord, *Surface and Interface Analysis* 34 (1) (2002) 494–497.
- [14] J. Huot, I. Swainson, R. Schulz, *Annales de Chimie Science des Matériaux* 31 (1) (2006) 135–144.
- [15] R.A. Varin, et al., *Journal of Alloys and Compounds* 432 (2007) 217–231.